Journal of Catalysis 267 (2009) 14–23

Contents lists available at ScienceDirect

Journal of Catalysis

journal homepage: www.elsevier.com/locate/jcat

Effect of NTA addition on the structure and activity of the active phase of cobalt-molybdenum sulfide hydrotreating catalysts

M.A. Lélias [a,1], P.J. Kooyman [b], L. Mariey [a], L. Oliviero [a], A. Travert [a], J. van Gestel [a], J.A.R. van Veen [c], F. Maugé [a,*]

[a] Laboratoire de Catalyse et Spectrochimie, Université, Ensicaen, CNRS, 6 bvd Maréchal Juin, 14050 Caen, France
[b] DelftChemTech, Delft University of Technology, Julianalaan 136, 2628 BL Delft, The Netherlands
[c] Shell Research and Technology Centre Amsterdam, P.O. Box 38000, 1030 BN Amsterdam, The Netherlands

ARTICLE INFO

Article history:
Received 3 May 2009
Revised 15 July 2009
Accepted 15 July 2009
Available online 22 August 2009

Keywords:
Hydrotreatment
Chelating agent
Nitrilo triacetic acid
NTA
IR spectroscopy
Carbon monoxide

ABSTRACT

CoMoS catalysts with constant Co and Mo contents were prepared with different amounts of nitrilo triacetic acid (NTA) chelating agent. NTA has a marked positive effect on the catalyst activity for gas-phase reactions such as atmospheric pressure thiophene hydrodesulfurization (HDS) and high-pressure 2,6-dimethyl aniline hydrodenitrogenation, whereas no effect is found for liquid-phase dibenzothiophene HDS. Transmission electron microscopy analysis shows that NTA has no effect on MoS_2 slab size and stacking, while infrared spectroscopy of adsorbed CO reveals a strong increase in the amount of Co-promoted sites. Comparison of activity and spectroscopic data implies that increase of Co-promoted sites accounts for the catalytic activity enhancement, but it also provides evidences for the creation of different kinds of sites on the NTA catalysts. Various possibilities (type II CoMoS phase, Co clusters, or CoMoSN) are discussed.

© 2009 Elsevier Inc. All rights reserved.

1. Introduction

To limit polluting emissions and preserve the catalytic converter from poisoning, more drastic regulations have been issued to limit the sulfur content in fuels. Hydrotreatment is the most widely used process to remove sulfur from oils. Hydrotreating catalysts are generally composed of small MoS_2 crystallites promoted by cobalt (or nickel) dispersed on alumina-based supports [1]. The anchoring of Co atoms on the edges of the MoS_2 slabs (CoMoS sites) accounts for the creation of active sites, whereas cobalt can also be present as a separate CoS_x phase or as spinel in the support [2]. By comparing catalytic data and sulfide slab size measured by transmission electron microscopy (TEM), Kastzelan et al. proposed a hexagonal shape for the sulfide slabs of alumina-supported CoMo catalysts [3]. This geometrical model has been largely used as a base for quantification of the amount of edge sites [4]. Recent scanning tunneling microscopy (STM) observations of sulfide slabs deposited on flat gold surfaces show that unpromoted Mo sulfide slabs are triangular, whereas after Co deposition the sulfide slabs become hexagonal [5]. Further investigations also differentiated two types of CoMoS phase, called type I and type II [1,3–5], which are distinguishable by their sulfidation degree and by differences in their interaction with the carrier. The CoMoS phase of type II, with lower interaction with the support, is generally the most active one.

Several preparation routes were developed in order to improve the performance of hydrotreating catalysts. In 1986, a patent from Shell was the first to describe the use of chelating agents such as nitrilo triacetic acid (NTA) to improve the catalytic performances of CoMo and NiMo catalysts [6]. NTA [8–10] is still the most widely used chelating agent along with ethylene diamino tretraacetic acid (EDTA) [7,8] and cyclohexane diamine tetraacetic acid (CyDTA) [5,8–12]. An increase of thiophene hydrodesulfurization (HDS) activity is generally reported when these chelating agents are present during catalyst preparation, although the extent of increase differs strongly between different publications. For HDS of dibenzothiophene (DBT), a test performed in more drastic conditions (under high pressure and in the liquid phase), Hiroshima et al. [9] have shown an activity increase when the $CoMo/Al_2O_3$ catalysts are prepared using EDTA or CyDTA, whereas no influence of NTA addition was observed. Van Veen at al. [10] even found a slight decrease of the DBT HDS activity of $NiMo/Al_2O_3$ catalyst when NTA was added. It appears that a ratio of NTA/metal close

* Corresponding author. Fax: +33 231 45 28 22.
E-mail address: francoise.mauge@ensicaen.fr (F. Maugé).
[1] Present address: Axens – Usine de Salindres, BP 8, 30340 Salindres, France.

0021-9517/$ - see front matter © 2009 Elsevier Inc. All rights reserved.
doi:10.1016/j.jcat.2009.07.006

to one [11] and the absence of a calcination step before sulfidation are key points to obtain more active catalysts, but the activation stage and catalytic test conditions can also affect the effect of chelating agent addition.

To specify the effect of chelating agents on the sulfide slab structure, various studies were undertaken. Hensen et al. [12] as well as Okamoto et al. [13] used TEM to study the effect of NTA on Mo/Al_2O_3 catalysts. They both found an increase of the length and stacking of the MoS_2 slabs. For $CoMo/Al_2O_3$ catalysts, Gonzalez-Cortés et al. [7] showed that the addition of EDTA also induces an increase of the average slab length. These results are in contradiction with those reported by Hiroshima et al. [9], who used extended X-ray absorption fine structure in order to compare the dispersion of Mo on a $CoMo/Al_2O_3$ catalyst with or without NTA and concluded that Mo dispersion was independent of the presence of the chelating agent.

Shimizu et al. [8] used infrared (IR) spectroscopy of adsorbed NO on sulfided CoMo catalysts prepared with or without chelating agents such as NTA and EDTA in order to determine the promotion of the sulfide phase by Co. They showed that catalysts with or without chelating agents have comparable total numbers of sites, but have more exposed Co atoms when prepared with a chelating agent. Kubota et al. [14] followed the chelating agent effect using EXAFS and showed that NTA induces, after sulfidation, a decrease of the quantity of Co in inactive form.

Hence, the effect of chelating agent on the dispersion and nature of the sulfide phase in the presence of chelating agent seems controversial. Different hypotheses are reported to explain the origin of the effect of chelating agent addition. Medici et al. [15] attribute the positive influence of chelating agent to the stability of the promoter-chelating agent complex at high temperature toward the H_2S/H_2 mixture. Similarly, de Jong et al. [16] and Coulier et al. [17,18] used model catalysts to study the effect of NTA on the sulfidation temperatures of the different metals, and concluded that NTA delays the sulfidation of cobalt to temperatures at which MoS_2 is already formed. However, IR analysis of the sulfide phase formed on supported sulfide catalysts does not confirm this conclusion [11]. Another proposal based on Mössbauer results is that NTA favors the formation of type II CoMoS [19,20].

Hence, the literature shows some discrepancies concerning chelating agent effect, but the various types of preparations and the different methods of sulfidation used hamper understanding the effect of chelating agent on the formation and structure of the sulfide phase.

The objective of the present study is to determine the role of NTA on the change of activity and functionalities of the catalysts more systematically, and to relate these changes to the structure and concentration of active sites.

To this aim, a set of NTA–$CoMo/Al_2O_3$ catalysts with constant Co and Mo contents and increasing NTA amount was studied. Taking into account the previous studies, the chelating agent was added together with the metals during the incipient wetness impregnation. After drying, the catalyst was directly sulfided (without calcination step). The effect of NTA was tested in three different catalytic tests: thiophene HDS, which is commonly used for a rapid evaluation of the catalytic performance, HDS of dibenzothiophene (DBT), which is currently used in both industrial and academic laboratories as a representative test for HDS of diesel, and 2,6-dimethylaniline (DMA) decomposition which enables evaluation of the various catalytic functions [21]. Note that thiophene HDS and DMA HDN are gas-phase reactions, while DBT HDS is carried out in the liquid phase. The structure as well as the nature and amount of sulfide phase of the NTA catalysts was characterized using IR spectroscopy of CO adsorption [22,23] and HREM.

2. Experimental

2.1. Catalyst preparation

The catalysts were prepared by pore-volume impregnation of a γ-alumina ($S_{BET} = 258\ m^2\ g^{-1}$; $V_{porous} = 0.66\ cm^3\ g^{-1}$) according to the procedure developed by van Veen et al. [20]. The NTA was introduced together with the metallic precursors. Different solutions containing cobalt(II)nitrate ($Co(NO_3)_2{\cdot}6H_2O$, Merck), ammonium heptamolybdate ($(NH_4)_6Mo_7O_{24}{\cdot}4H_2O$, Merck), and NTA ($[C_2H_3O_2]_3N$, Acros Organics) were prepared in order to obtain catalysts containing 2.1 wt% Co, 10 wt% Mo, and various amounts of chelating agent (0, 0.25, 0.9, and 1.2 mol of NTA/mol of metal (Co + Mo)). The solution was added to the carrier and shaken vigorously. Subsequently the preparation was put on a roller bank for 30 min and dried indirectly with the help of a hair dryer at 393 K for 1 h. Before sulfidation, the catalysts were not calcined but only dried at 393 K in order to keep the chelating agent in its initial form. The catalysts are denoted as CoMox.xxNTA, where x.xx is the molar ratio NTA/(Co + Mo).

2.2. Weight of the working catalyst

The weight of the working catalyst was experimentally determined in order to take into account the important mass loss that occurs during sulfidation stage, i.e. water elimination, molybdenum and cobalt precursors sulfidation, and NTA decomposition [24]. The weight loss upon sulfidation (according to the thiophene test procedure) is compared to the amount of NTA introduced in the catalysts (Fig. 1). The weight loss determined experimentally is generally greater than that expected considering only the NTA decomposition (dotted line). These discrepancies decrease when the NTA amount increases. This indicates a lower moisture content on the NTA-containing catalysts and suggests that the presence of NTA on the alumina support hinders water adsorption. In all the following sections, the weight of the catalysts is the weight of the sulfided catalysts.

2.3. Thiophene hydrodesulfurization

The thiophene HDS activity test was carried out in a flow microreactor working at atmospheric pressure and 623 K. Appropriate amounts of catalysts (about 20 mg) were used in order to keep the conversion lower than 5%. Before the reaction, the catalysts

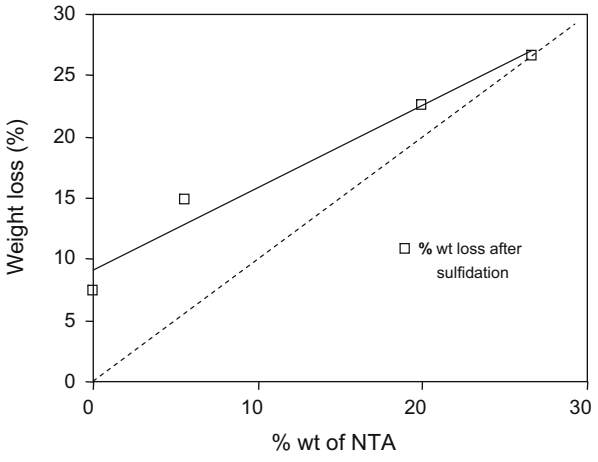

Fig. 1. Catalyst weight loss measured after sulfidation of the different NTA catalysts. The dotted line corresponds to the expected weight loss only due to NTA decomposition.

were sulfided *in situ* with 30 mL min^{-1} of H_2S/H_2 (10 vol%) at 623 K (heating rate of 3 K/min) for 30 min.

Thiophene was introduced into the reactor by flowing hydrogen (70 mL min^{-1}) through a thiophene saturator maintained at 291 K and mixed into 20 mL min^{-1} of H_2S/H_2 (10 vol%). Products were analyzed on-line using a Varian gas chromatograph equipped with a flame ionization detector (FID) and CPSIL-5CB capillary column. The specific rate was calculated as $r_{HDS} = (F/m)X$, where F/m is the molar flow rate of reactant per gram of catalyst and X is the thiophene conversion.

2.4. Dibenzothiophene hydrodesulfurization

High-pressure liquid-phase DBT HDS measurements [10] were performed in a 6-parallel nanoflow reactor system. About 400 mg of catalyst (diluted with 1.2 g of SiC) was sulfided *in situ*. First, the catalyst was wetted with a mixture of hexadecane and 3 wt% of di-tertiononyl pentasulfide (TNPS) with a flow of 0.75 mL h^{-1} before a flow of 135 mL h^{-1} of H_2 was added. The catalysts were heated to 373 K, and the pressure was raised to 3.5 MPa. Then, the temperature was raised to 553 K with a rate of 0.33 K/min, and maintained for 5 h. Then it was raised again to 613 K with a rate of 0.33 K/min, and maintained for 24 h. Finally, the reactor was cooled down to 473 K in 2 h.

The feed was a mixture of DBT (5.00 wt%), marker paraffin (C_{12}) (1.72 wt%), and hexadecane (93.28 wt%). The flow of the feed was 0.75 mL h^{-1} and the flow of H_2 was 2.25 mL min^{-1}. Activity was measured at 493 K, 503 K, 518 K, and 533 K for periods of 20 h. The products (biphenyl, cyclohexylbenzene, and unreacted dibenzothiophene) were analyzed with a Carlo Erba Instrument ICU 600 gas chromatograph equipped with a FID.

2.5. 2,6-Dimethylaniline hydrodenitrogenation

The 2,6-dimethylaniline HDN activity test was carried out in a stainless steel reactor (Sotelem) at 4 MPa and 573 K. Around 0.35–0.40 g of catalyst was first sulfided *in situ* under 60 mL min^{-1} of H_2S/H_2 (10 vol%) at 4 MPa at 623 K for 2 h (temperature ramp 3 K/min). Thereafter, the catalyst was cooled under H_2S/H_2 to the reaction temperature, and the H_2S content adjusted to 1.4% in hydrogen. The liquid feed (10 vol% 2,6-dimethylaniline, reactant; 80% heptane, solvent; and 10% decane, internal standard) was introduced using an HPLC pump and vaporized in the H_2S/H_2 stream. The reaction products were condensed at the reactor exit, and the liquid was analyzed using a Varian gas chromatograph equipped with a CPSIL-5CB capillary column and a FID detector.

The partial pressure of 2,6-dimethylaniline was kept constant at 13 kPa for all experiments. Reaction conditions at steady state were varied by changing the contact time (55–250 h g mol^{-1}) at 56 or 0 kPa of H_2S. We determined the reaction orders in 2,6-dimethylaniline for the hydrogenation (HYD), xylene (XYL), and disproportionation (DIS) routes as 0.0, 0.0, and 0.4, respectively [21]. Activities are expressed by the initial rates, i.e. reaction rates at zero conversion (mol h^{-1} kg^{-1}).

2.6. IR spectroscopy of adsorbed CO

2.6.1. IR experiments

Before introduction into the IR cell, the samples were ground and pressed to obtain a wafer (area 2 cm^2, mass about 10 mg, but precisely weighed). The spectra were recorded using a Fourier Transform IR spectrometer from Thermo Optek using a MCT detector. Spectra were recorded with 256 scans at a resolution of 4 cm^{-1}. All the spectra presented in this paper are normalized to a disc of 5 mg cm^{-2} of sulfided catalyst.

2.6.2. Standard sulfidation procedure

A standard sulfidation was carried out *in situ* in the IR cell according to the following procedure. The disc was sulfided under a flow of H_2S/H_2 (10/90) at 30 mL min^{-1}, with a heating rate of 10 K/min up to 543 K, and then maintained at this temperature for 30 min. The temperature was then raised to 623 K and maintained for 2 h. After 1 h30 at this temperature, the H_2S/H_2 flow was stopped and replaced by a flow of N_2 at 30 mL min^{-1} for 30 min. Then, the sample was cooled down to room temperature under N_2. Afterward, an evacuation was performed from RT to 573 K (with a rate of 10 K/min) and maintained at 573 K until a pressure of 10^{-3} Pa was reached. Finally, the sample was cooled down to liquid nitrogen temperature before CO introduction.

2.6.3. H_2 post-treatment procedure

In some cases after standard sulfidation, the sample was submitted to a H_2 post-treatment. Thus, after standard sulfidation at 623 K, N_2 flush and evacuation at 573 K (described in the previous section), a first dose of 13.3 kPa of H_2 was introduced into the IR cell. After 30 min of H_2-contact at 573 K, the cell was evacuated, and the catalyst was contacted with a second dose of 13.3 kPa of H_2 for 30 min. The cell was evacuated under secondary vacuum at 573 K, and cooled down to liquid nitrogen temperature.

2.6.4. Procedure for CO adsorption

Before CO introduction, a reference spectrum of the activated catalysts was recorded at 100 K. Then, small calibrated doses of CO were introduced until an equilibrium pressure of 133 Pa was established. A spectrum was taken after each CO introduction. All the CO spectra presented correspond to difference spectra, i.e. spectrum after CO adsorption minus reference spectrum.

2.6.5. Spectral analysis

The concentration of each type of sites was calculated using spectral decomposition. For sulfided CoMo, the CO adsorption zone of the spectrum was fitted using five Gaussian curves corresponding to: CUS Al^{3+}(2186 cm^{-1}), Al–OH (2153 cm^{-1}), MoS_2 sites (2109 cm^{-1}), and CoMoS sites (2064 and 2028 cm^{-1}). The area of each band was then obtained using the fitting procedure of the OMNIC software. For all catalysts, the wavenumber of the band maximum and width at half height of the bands were kept in fixed limits. The detailed procedure with all the parameters used is given as Supplementary material on-line (http://www.elsevier.com.chimie.gate.inist.fr).

Calculation of the site concentrations was then done using the molar extinction coefficient determined previously ($\varepsilon_{MoCUS} = 16 \pm 4$ μmol^{-1} cm and $\varepsilon_{CoMoSCUS} = 43 \pm 12$ μmol^{-1} cm) [22].

2.7. Transmission electron microscopy

Quasi *in situ* high-resolution transmission electron microscopy (HREM) was performed using a Philips CM30T equipped with an LaB6 filament operated at 300 kV. To avoid detrimental exposure to air [25], sulfided catalysts were unloaded from the sulfidation reactor in a nitrogen glovebox. They were packed air-tight and transported to an argon glovebox near the microscopes, where they were mounted on Quantifoil® microgrid carbon film-covered metal TEM grids. A few drops of a suspension of ground catalyst in dry *n*-hexane were put on the TEM grid and left to dry inside the glovebox. Grids were transferred to the TEM using a specially developed protective-atmosphere transfer TEM holder [26].

Different procedures of sulfidation were used: (i) gas phase under 1 bar of H_2S/H_2; (ii) liquid phase under 40 bars in the presence of TNPS and heptane (same procedure as used for sulfidation in the DBT test); and (iii) gas phase under 40 bars of H_2S/H_2, this sulfidation was only performed on the catalyst without NTA.

Slab length and stacking degree distributions of sulfide slabs were determined manually by measuring at least 300 slabs per sample from the TEM images. Average slab length and fraction of Mo at the edges of the slabs were calculated from the slab length distributions, assuming MoS_2 crystallites of hexagonal morphology [3,12].

3. Results

3.1. Catalytic activity of the NTA catalysts

3.1.1. Hydrodesulfurization of thiophene

Thiophene HDS shows that NTA addition leads to a marked increase of the HDS activity of the $CoMo/Al_2O_3$ catalyst (by a factor of ~2.6) (Fig. 2). The literature generally reports a beneficial effect of NTA addition in thiophene HDS although the extent of this positive effect is lower than that measured in the present work [27].

3.1.2. Hydrodesulfurization of dibenzothiophene

In the case of HDS of DBT, the addition of NTA does not modify the conversion or the selectivity whatever be the temperature of reaction (493–530 K).

3.1.3. Hydrodenitrogenation of 2,6-dimethylaniline

As shown previously [21], DMA is decomposed according to four parallel routes: dearomatization followed by (ia) hydrogenation – elimination to dimethylcyclohexenes and dimethylcyclohexanes (HYD) or (ib) NH_3 elimination to *m*-xylene (HYG), (ii) direct NH_3 elimination from DMA to *m*-xylene (DDN) (mainly observed in the absence of H_2S), and (iii) disproportionation of DMA to 2-methylaniline and 2,4,6-trimethylaniline (DIS). In the discussion, we will refer to XYL activity as the formation of xylene by both the HYG and DDN routes. To explore the full potentialities of the catalysts, the HDN test was performed either in the presence or in the absence of H_2S.

3.1.3.1. Effect of NTA on HYD activity. Fig. 3A shows that the HYD activity of the catalysts increases with the amount of NTA. This augmentation is less important than that measured for thiophene HDS. Indeed, the HYD activity measured in the presence of H_2S is increased by a factor of ~1.5 for the highest NTA loadings. The HYD activities are increased by the absence of H_2S, and the extent of this augmentation is independent of the NTA amount (except in the absence of NTA where no increase is observed in the absence of H_2S) (Fig. 3A).

3.1.3.2. Effect of NTA on XYL activity. Fig. 3B shows that the XYL activity increases upon NTA addition. However, the influence of H_2S partial pressure is markedly dependent on the level of NTA present. The calculated ratio between the XYL activities measured in the absence and in the presence of H_2S strongly increases with the NTA content: the ratio is 1.3 for the catalyst without NTA, and it increases up to 2.8 for the highest NTA loadings.

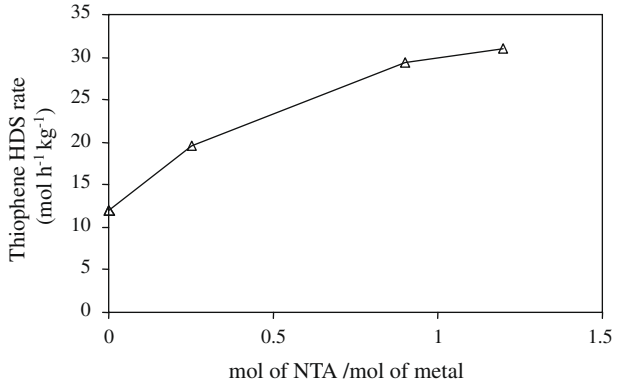

Fig. 2. Thiophene HDS activity of the various NTA catalysts.

3.1.3.3. Comparison between HYD and XYL activities. Fig. 4 shows that the influence of H_2S partial pressure differs significantly for the XYL and HYD routes, and for catalysts with and without NTA. In the presence of H_2S, a linear relationship is found between the XYL and HYD routes (increase of both routes by a factor of ~1.5) suggesting that under these conditions HYD and XYL proceed via the same intermediate [21]. By contrast, without H_2S the XYL activity increases more strongly than the HYD activity when increasing the NTA amount, and no linear relationship appears between the two routes (Fig. 4).

3.1.3.4. Effect of NTA on DDN route. As reported previously [24,28], the strong increase of the XYL/HYD ratio in the absence of H_2S was assigned to a second route for xylene formation, DDN. Hence, from the total XYL formed in the absence of H_2S and taking into account the ratio HYD/XYL measured in the presence of H_2S, the additional xylene formed via the DDN route in the absence of H_2S can be calculated. Fig. 5 shows that the DDN activity increases linearly with NTA content.

3.1.4. Comparison of the NTA effect in the different catalytic tests

Addition of NTA to the $CoMo/Al_2O_3$ catalyst leads to an increase of the thiophene HDS activity as well as of DMA HDN. The thiophene activity can be increased by a factor of 2.6, while this factor amounts to about 1.5 for the HYD and XYL routes in the presence of H_2S. In the absence of H_2S, a strong DDN activity is developed, which increases with NTA content.

A linear relationship exists between thiophene HDS activity and HYD activity in the presence of H_2S (Fig. 6). This indicates that, on this set of catalysts, thiophene HDS and DMA HYD probe the same type of sites. This activity enhancement provides evidence for an increase of the amount of CoMoS sites with NTA addition.

As shown previously [21], the DDN route, i.e. the direct ammonia elimination (without previous hydrogenation), requires highly unsaturated unpromoted Mo sites. Hence, the increase of the DDN route observed on NTA-containing catalysts is surprising. Indeed, the increased concentration of Co-promoted sites with NTA addition indicated by DMA HYD and thiophene HDS should lead to a diminution of the amount of unpromoted Mo sites, and consequently to a decrease of the DDN activity. A reverse trend is observed that indicates the development of new types of sites on NTA catalysts.

For DBT HDS (not shown), NTA addition does not lead to any activity increase. Note that the absence of any positive effect in HDS of DBT has been reported already by van Veen et al. for NTA addition to $NiMo/Al_2O_3$ catalysts [10]. It should be mentioned that the sulfidation procedures used for DBT HDS and DMA or thiophene tests are completely different. The sulfiding agent TNPS used in DBT HDS might mask any effect of NTA by leading to a high promotion level even in the absence of NTA. On the other hand, it has been reported already that NTA only promotes HDS and HDN in the gas phase but not in the liquid phase [28].

3.2. Nature and concentration of the sulfide-phase sites of the NTA catalysts

3.2.1. Residual organic species after sulfidation

IR spectra presented in Fig. 7 show bands at 1608, 1580, 1471, and 1300 cm^{-1} to be present after sulfidation of the NTA catalysts at 623 K. The intensity of the three latter bands increases with the

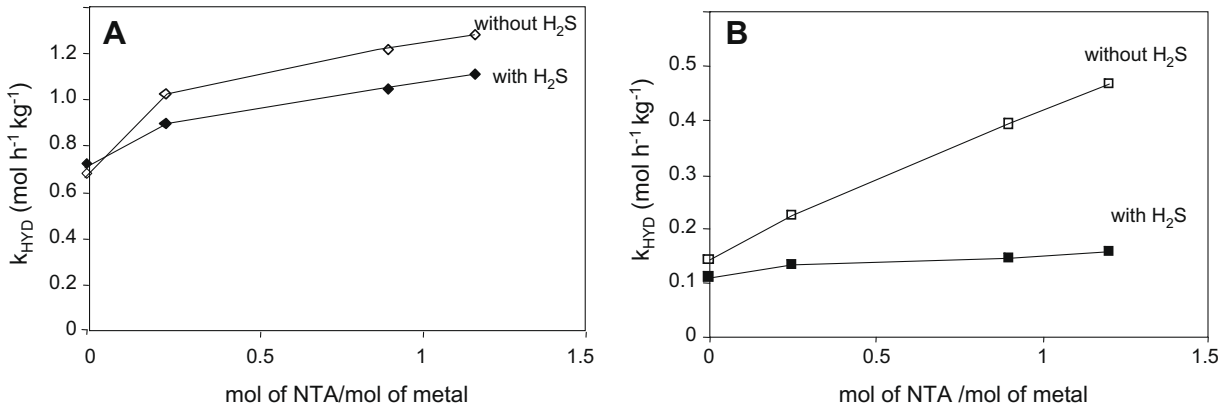

Fig. 3. HDN activity of the various NTA catalysts measured in the presence of H_2S (56 kPa) or in the absence of H_2S: (A) HYD activity; (B) XYL activity.

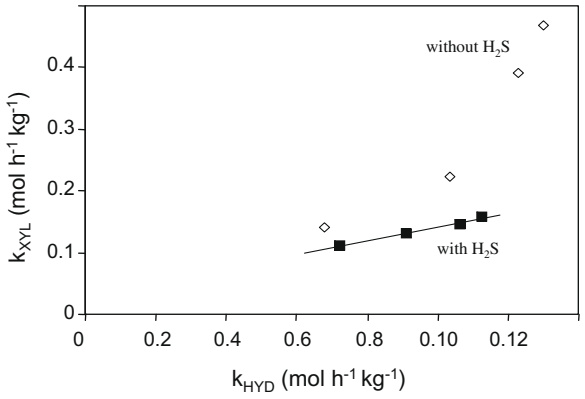

Fig. 4. Relationship between XYL and HYD activities measured in the presence and in the absence of H_2S.

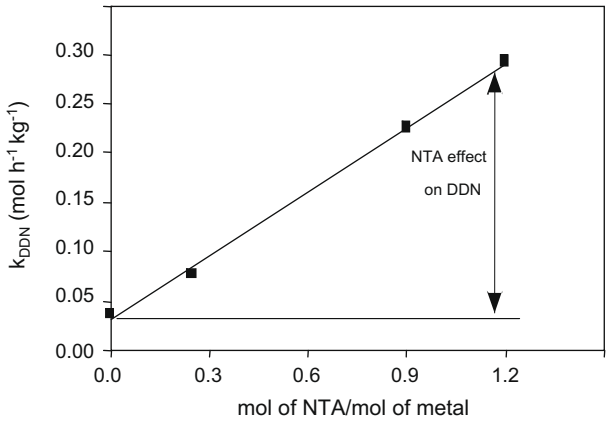

Fig. 5. Rate constant of the DDN route of the various NTA catalysts measured in the absence of H_2S.

NTA amount. The 1608 cm^{-1} band is more specifically observed on the catalysts containing the highest amount of NTA. These bands are close to those observed after treatment of NTA deposited on pure Al_2O_3 under vacuum at 623 K (see inset Fig. 7). These species can correspond to carboxylate adsorbed on Lewis acid sites of alumina. Thus, some residual organic fragments issued from NTA decomposition are still present on the alumina surface after sulfidation of the NTA catalysts at 623 K. Note that these species are still observed after sulfidation followed by H_2 treatment at 523 K.

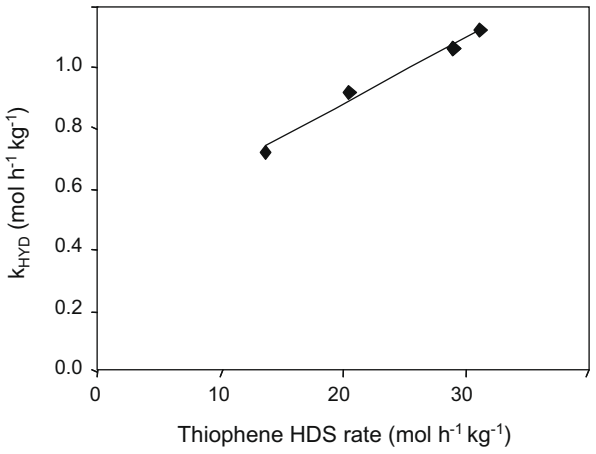

Fig. 6. Comparison between the rate constants for HYD route of DMA decomposition measured in the presence of 56 kPa H_2S and for thiophene HDS.

3.2.2. CO adsorption on sulfide phase

In order to determine the NTA effect on the nature and amount of the sulfide sites, IR analysis of CO adsorption was performed on sulfided as well as on H_2 post-treated NTA catalysts (in order to mimic the atmosphere of DMA decomposition without H_2S).

IR spectroscopy of CO adsorbed on sulfided CoMo catalysts (not presented) shows a band at ~2070 cm^{-1} characterizing CoMoS sites and one at ~2110 cm^{-1} associated to unpromoted Mo sites [22,29]. After H_2 treatment, similar types of sulfide sites are detected (Fig. 8). Just as after sulfidation, no noticeable band shift due to NTA addition can be evidenced after H_2 treatment.

On sulfided catalysts as well as on H_2-treated ones (Fig. 9A and B), CO adsorption shows that NTA addition, up to 0.9 mol NTA/mol metal, strongly increases the concentration of Co-promoted sites. For the highest NTA content (1.2 mol NTA/mol metal), the amount of CoMoS sites stays almost constant. The amount of unpromoted Mo sites is not significantly modified by NTA addition. Hence, the degree of promotion of the sulfide phase (PD, i.e. concentration of CoMoS sites over concentration of (CoMoS + Mo sites)) is multiplied by 1.4 by NTA addition (Table 1 – increased from 0.43 to 0.61). It should be noted that the total amount of sulfide-phase sites detected by CO increases with the NTA content.

The ratio between the amount of sites detected after H_2 treatment and after sulfidation is presented in Table 1 (values in parentheses). H_2 treatment strongly increases the CO uptake on the sulfide phase. Indeed, H_2 treatment eliminates some sulfur atoms via H_2S formation, creating supplementary CUS on the sulfide phase. Note that for CoMoS sites this ratio decreases significantly

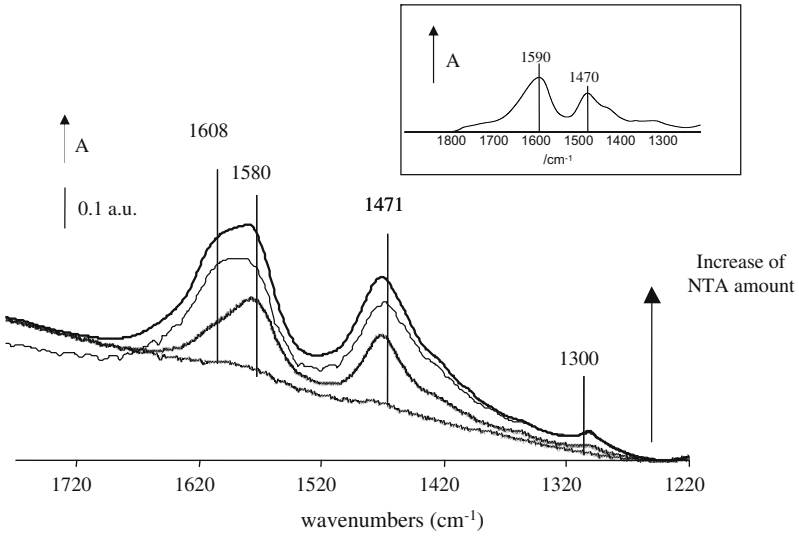

Fig. 7. IR spectra of the various NTA catalysts after sulfidation at 623 K. Inset: NTA–Al_2O_3 after sulfidation at 623 K.

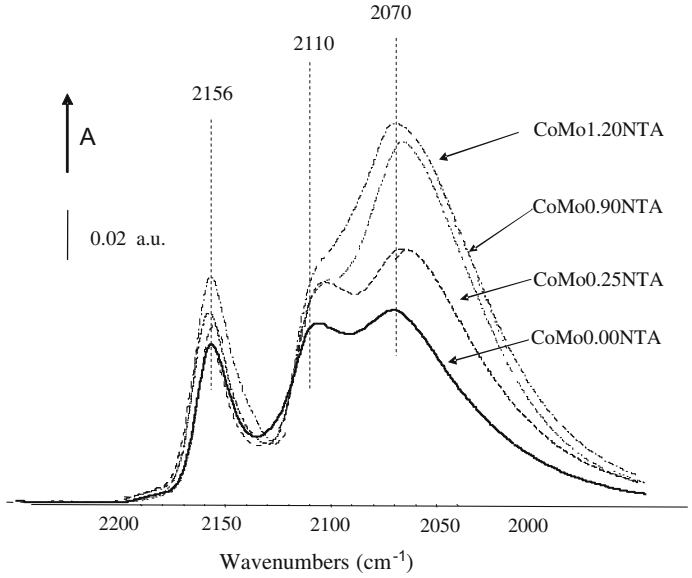

Fig. 8. IR spectra of CO adsorbed on the NTA catalysts after H_2 post-treatment.

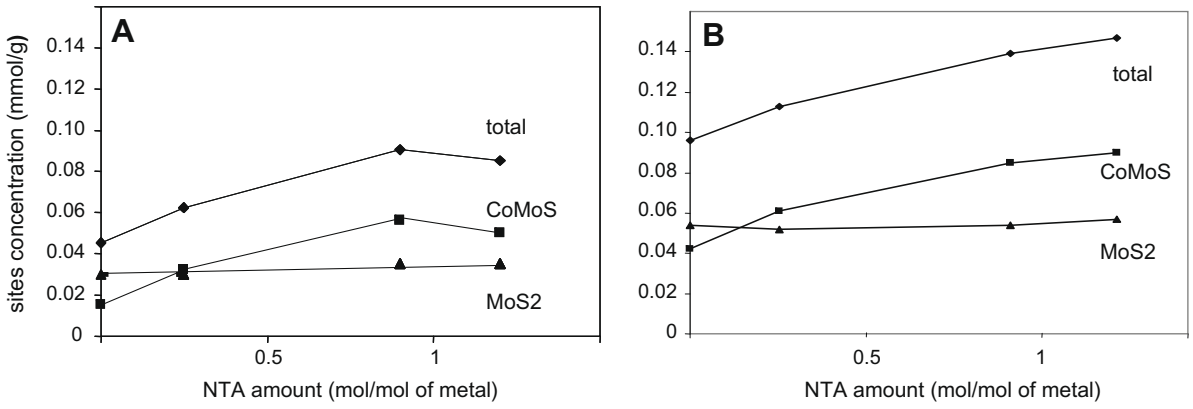

Fig. 9. Variation of the amount of Mo, CoMoS, and total sites with the amount of NTA. (A) Sulfided catalysts. (B) Sulfided catalysts after H_2 treatment.

Table 1
Amount of promoted, unpromoted Mo, and total sites, and promotion degree determined from CO adsorption after H_2 treatment of the sulfided catalysts.

Catalyst	*n* MoS_2sites (μmol/g)	*n* CoMoS sites (μmol/g)	*n* total sites (μmol/g)	Promotion degree*
CoMo0.00NTA	54 (1.8)**	42 (2.6)	96	0.43
CoMo0.25NTA	52 (1.7)	61 (2.1)	113	0.54
CoMo0.90NTA	54 (1.5)	85 (1.5)	139	0.61
CoMo1.20NTA	57 (1.6)	90 (1.8)	147	0.61

* Promotion degree = *n*(CoMoS sites)/*n*(total sites).
** In parenthesis – H_2 treatment effect calculated from *n*(sites after H_2 treatment)/*n*(sites after sulfidation).

when NTA is added, as it goes from 2.6 on CoMo0.00NTA to 1.8 on CoMo1.20NTA.

To sum up, addition of NTA strongly increases the amount of CoMoS sites (by a factor of ~2). Maximum of promoted sites is obtained for an amount of 0.9 mol NTA per mol of metal. In addition, different points suggest some changes in the environment of the sulfide sites with NTA, as an increase of the total amount of sulfide-phase sites and the modifications of the extent of the H_2 effect.

3.3. Effect of NTA addition and sulfidation pressure on the morphology of sulfide phase

In order to determine the effect of NTA on the dispersion and stacking of the sulfide phase, the sulfided NTA catalysts were characterized using quasi *in situ* TEM. Different procedures of sulfidation were used: (i) gas phase under 0.1 MPa of H_2S/H_2; (ii) liquid phase under 4 MPa in the presence of TNPS and hexadecane; and (iii) gas phase under 4 MPa of H_2S/H_2. These different procedures mimic the various sulfidation conditions used in the different reactivity tests.

The length and the stacking distributions of the sulfide phase obtained after atmospheric pressure sulfidation are presented in Fig. 10A. For all the NTA catalysts, the average length is about 2.6 nm and the stacking is about 2. NTA addition has a negligible effect on the distributions of length and stacking.

The morphology of the NTA catalysts sulfided in the liquid phase is presented in Fig. 10B. As observed previously, NTA addition hardly induces differences in the average values and in the distributions of the slab length and stacking. However, this sulfidation procedure clearly increases the average length of the sulfide slabs compared to the atmospheric pressure sulfidation (3.6 instead of 2.6 nm), whereas the stacking is not modified (about 2).

In order to discriminate the influence of the sulfidation pressure from that of the sulfiding agent, the morphology of the CoMo0.00NTA catalysts sulfided under high pressure and TNPS was compared to that obtained after sulfidation under high pressure

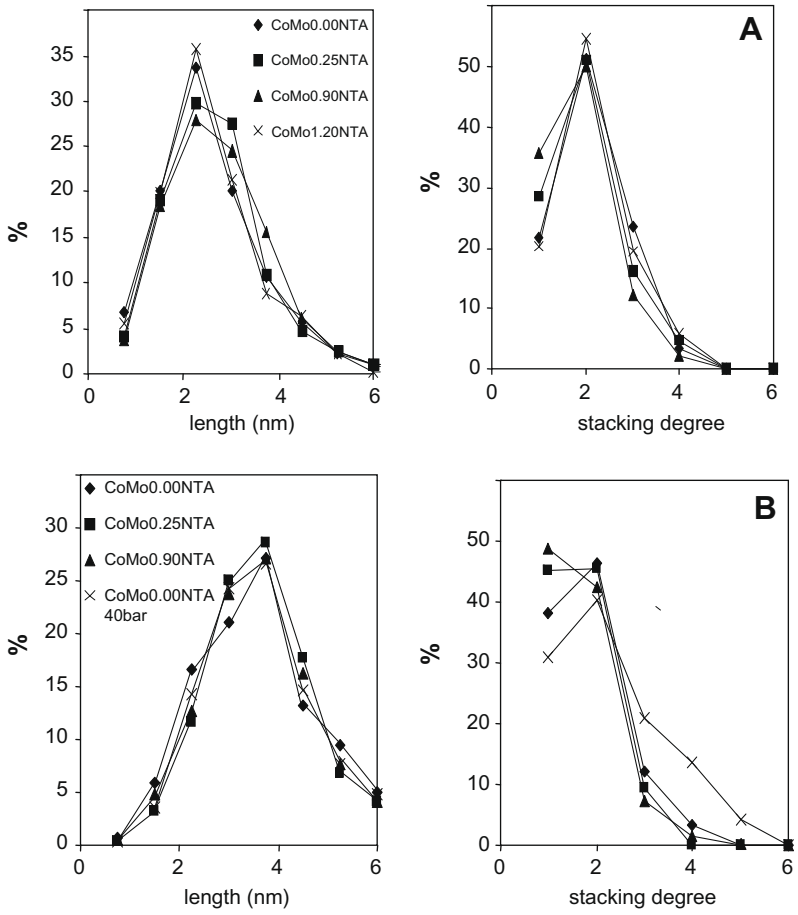

Fig. 10. TEM analysis of the morphology of the sulfided NTA catalysts – (A) Sulfidation under 1 bar H_2S/H_2. (B) Sulfidation under 40 bars of TNPS and heptane (for all the catalysts) or under 40 bars of H_2S/H_2 (for CoMo0.00NTA).

and H_2S/H_2. Fig. 10B shows that the sulfidation pressure is the main parameter which affects the dispersion of the slabs. Indeed, using of a gas-phase sulfidation instead of a liquid-phase sulfidation (both at 4 MPa) does not change the average slab length. Note that the change of sulfiding agent leads to some modifications in the stacking, i.e. the average slab stacking reaches 2.5 in the case of H_2S instead of 2 for TNPS.

In conclusion, the sulfidation procedure (pressure and sulfiding agent) significantly influences the morphology of the sulfide phase. Increasing the pressure leads to longer slabs, but it hardly changes the stacking. Changing the sulfiding conditions (liquid phase vs. gas phase) can change the stacking. However, for similar procedures of sulfidation, NTA addition modifies neither the length nor the stacking of the slabs.

4. Discussion

4.1. Influence of NTA on the catalytic activity

4.1.1. Effect of NTA on the active sites for thiophene HDS

Comparison of thiophene HDS activity of the various NTA catalysts to the concentration of CoMoS sites measured after sulfidation (Fig. 11) reveals a linear relationship between the HDS activity and the amount of CoMoS sites. Hence, these results confirm that mainly the Co-promoted sites are responsible for the HDS activity.

4.1.2. Effect of NTA on the active sites for DMA hydrogenation

A similar comparison was plotted for the DMA reaction. For the HDN reaction, activity was measured in the presence or in the absence of H_2S. In parallel, site concentrations were determined on sulfided catalysts and on H_2-treated catalysts. Fig. 12 compares the hydrogenation rate measured in the presence of H_2S to the concentration of CoMoS sites detected after sulfidation (full symbols), and the hydrogenation rate measured in the absence of H_2S to the concentration of CoMoS sites detected after H_2 treatment (open symbols).

As shown in Fig. 12, a good correlation appears between the hydrogenation rate and the concentration of CoMoS sites (except for CoMo0.00NTA in the absence of H_2S). Note that the Co-promoted sites created by H_2 treatment have the same intrinsic activity in hydrogenation as those detected on sulfided catalysts. These results are in agreement with previous observations on a series of CoMo catalysts without NTA [30]. This indicates the absence of important changes in the environment of Co-promoted sites on sulfided catalysts by H_2 treatment. Hence, these results confirm that mainly the Co-promoted sites are responsible for the hydrogenation route of the DMA decomposition.

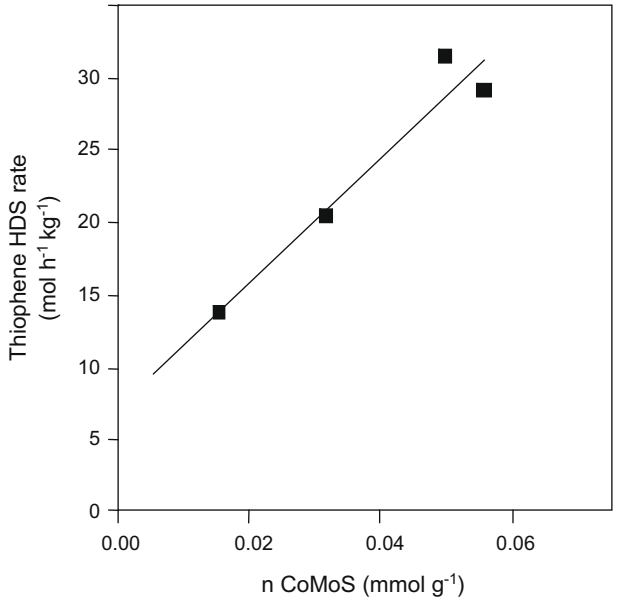

Fig. 11. Comparison between the thiophene HDS activity and the concentration of CoMoS sites.

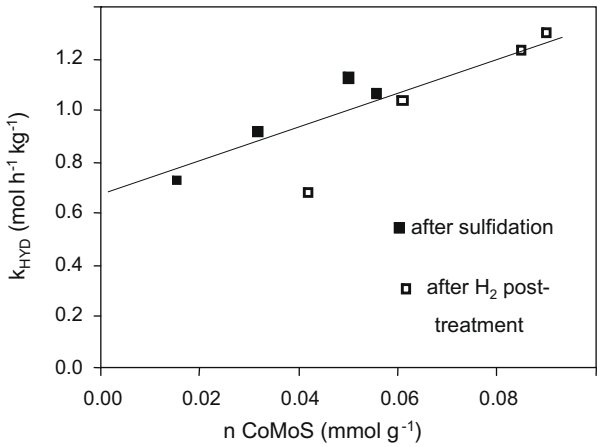

Fig. 12. Comparison between HYD activity route of DMA decomposition and concentration of CoMoS sites of NTA catalysts. Full symbol: activity measured in the presence of H_2S and concentration of sites detected after sulfidation. Open symbols: activity measured in the absence of H_2S and concentration of sites detected after H_2 treatment.

4.1.3. Effect of NTA on the active sites for DMA DDN route

NTA has been shown to increase the xylene formation via the DDN route (activity multiplied by a factor of 8). The active sites for the DDN route were thought to be highly unsaturated unpromoted Mo sites [30]. However, in the present study the concentration of unpromoted Mo sites stays almost constant when NTA is added. Moreover, a parallel appears between the concentration of Co-promoted sites and the DDN rate constant, even if the relationship is not linear (Fig. 13).

4.2. Influence of NTA on the nature of active sites

Even if previous section shows very good agreements between activity and amount of Co-promoted sites increases, one cannot exclude that NTA addition changes the nature of active sites. Only a quantitative analysis of catalytic and spectroscopic data could allow to answer this point. Hence, TOFs of the unpromoted and promoted NTA catalyst sites are calculated and compared to previous results obtained on CoMo series without NTA [30].

4.2.1. Effect of NTA on the nature of active sites for thiophene HDS

On the NTA series, the amount of unpromoted Mo sites is almost unchanged by chelating agent addition. Thus, an extrapolation of the line presented in Fig. 11 should correspond to the HDS activity of a pure Mo catalyst. The intercept is about 7 mol h^{-1} kg^{-1}. Therefore, the turn over frequency (TOF) value for Mo sites is about 230 h^{-1}. From the slope of the line relating HDS activity and amount of CoMoS sites, the TOF of these sites is equal to 435 h^{-1}. The values reported by Dujardin in [30] were 47 h^{-1} for Mo sites and 1080 h^{-1} for CoMoS sites. Although the thiophene HDS activities were measured at 673 K by Dujardin and at 623 K in this study, there is obviously a discrepancy between the two sets of results. Indeed, the effect of Co-promotion is markedly lower on the NTA series.

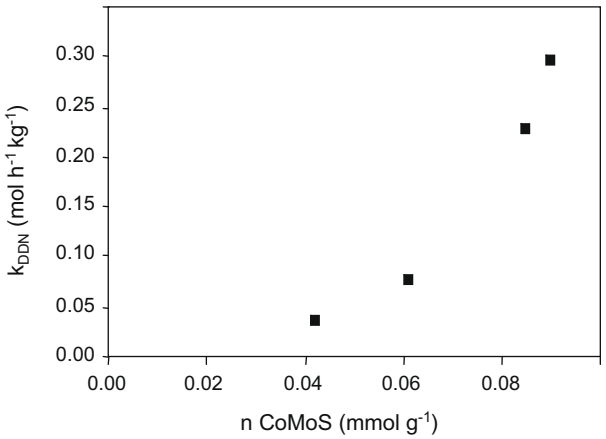

Fig. 13. DDN rate constant versus the concentration of CoMoS sites of the NTA catalysts.

4.2.2. Effect of NTA on the nature of active sites for DMA hydrogenation

The relation between HYD activity (in mol h^{-1} kg^{-1}) and concentration of CoMoS sites (in mmol g^{-1}) in Fig. 12 can be written as $k_{HYD} = 7^{*}n_{CoMoS} + 0.67$. This means that the TOF of the Co-promoted sites for the hydrogenation route of DMA amounts to 7 h^{-1} and that of the unpromoted Mo sites amounts to about 16 h^{-1}. The higher TOF value for the unpromoted sites as compared to the Co-promoted sites is highly unrealistic.

TOF values obtained by Dujardin et al. [30] were 16 h^{-1} and 1.5 h^{-1}, respectively, for CoMoS and Mo sites. These values are obtained at the same conditions for DMA test and using the same temperature of sulfidation before IR experiment but with a different protocol. Thus, for the series of $CoMo/Al_2O_3$ catalysts without additive [25], a more realistic factor of about 10 was found between the TOF values of promoted and unpromoted sites.

In the current study the unexpected relative values for the TOF of promoted and unpromoted sites can probably be explained by an artifact in the estimation of the concentration of sites. For this calculation, the same values for the molar extinction coefficients for the two types of sites have been used as in the work of Dujardin et al. [30]. The discrepancy in the TOFs obtained using the same molar extinction coefficients indicates that these values change upon addition of NTA. Therefore, from the combination of spectroscopic data and activity tests, we can conclude that the nature of the active sites is modified on NTA catalysts.

4.2.3. Effect of NTA on the nature of active sites for DMA DDN route

As described above, a change in the nature of Mo sites upon NTA addition could lead to an underestimation of their concentration. This could be proposed to explain the strong increase of DDN activity on NTA catalysts (factor of 8 for the highest NTA loading with respect to the NTA-free catalyst), whereas no change in the concentration of Mo sites is measured. If we consider a change of the CO/Mo molar extinction coefficient, it would mean that a factor of 8 is also needed, which seems not to be very probable.

The second hypothesis is related to the creation of a new type of Co-promoted sites. As suggested by Fig. 13, Co-promoted sites in a specific environment could be active for xylene formation via the DDN route.

4.3. Active sites on NTA catalysts

Activity and spectroscopic results show that the presence of NTA increases the amount of Co-promoted sites, leading to a marked enhancement of the catalytic activity in thiophene HDS and DMA HDN. However, some data also show that structural changes in the sulfide-phase sites occur with NTA. One can quote: (i) the increase of the total amount of adsorption sites detected by CO without change of dispersion of sulfide slab, (ii) the modification of sulfide site sensitivity to H_2 treatment evidenced from IR results, (iii) the HDS and HYD TOF values, and (iv) the increase of DDN activity with promotion degree increase. To sum up, some of the experimental data obtained on the NTA catalysts cannot be explained using only the decoration model, and activity results as well as quantitative IR data strongly suggest that formation of a new type of sites also occurs on the NTA catalysts. The change of concentration of the active sites as the only factor determining the activity increase must be excluded in view of the unrealistic TOF values. Thus, at least a part of the CoMoS sites must have been modified by NTA addition. However, we cannot specify which of the two features, i.e. increase of concentration or the change of quality of the CoMoS sites, is the major phenomenon that accounts for the increase of catalytic activity with NTA addition.

In fact, it should be noticed that quantification of the number of sites by IR spectroscopy of adsorbed CO on sulfide catalysts is rather delicate. Firstly, it is difficult to determine CO molar absorption coefficients for CoMo sulfide catalysts due to the simultaneous CO adsorption on both unpromoted and promoted sites. Secondly, different types of adsorption sites can give rise to the same CO frequency, and their absorption coefficients can be different. As shown in the Table 2, CO adsorbed on nitride or sulfide Mo catalysts can be difficult to discriminate. Nevertheless, the combination of CO adsorption with different reactivity tests gives useful information about the sulfide catalyst structure, via the TOF values.

For the modification of the CoMoS site quality, different possibilities can be considered.

4.3.1. Type II CoMoS phase

As mentioned in the introduction part, the presence of NTA, which decreases the interaction between the sulfide phase *in statu nascendi* and the subjacent carrier, could lead to the preferential formation of type II sulfide slabs. This proposal is strongly supported by the recent Mössbauer/XAS/DBT HDS study by Dugulan on similar catalysts [31]. Formation of type II sulfide phase could account both for the high performance of the NTA catalysts and for their modified behavior compared to conventional catalysts. Indeed, the presence of organic entities on the alumina surface could

Table 2
Comparison of the wavenumbers of CO adsorbed on various nitride catalysts.

Catalysts	Reference	Procedure of *in situ* activation	CO adsorption conditions	ν(CO) (in cm^{-1}) and proposed assignment
Mo_2N/Al_2O_3	Aegerter et al. [32]	Catalyst activated under H_2 at 750 K and evacuated at 673 K	CO adsorption at 130 K	2199 (Al^{3+}), 2165 (Mo), 2100 sh (Mo)
Mo_2N/Al_2O_3 Reduced and passivated	Yang et al. [33,34]	*In situ* synthesis under NH_3 flow at 873 K for 1 h	CO adsorption at 298 K	2200s (NCO), 2140–2090 sh ($Mo^{3+}(CO)_2$), 2045 sh ($Mo^{\delta+}$)
$CoMoN_x/Al_2O_3$	Yang et al. [34] Wu et al. [36,35]	*In situ* synthesis under NH_3 flow at 773 K for 1 h and evacuation at 773 K	CO adsorption at 298 K – contact during 10 min	2200 (NCO), 2155 w, 2060 ($Co^{\delta+}$), 2025 ($Mo^{\delta+}$)

modify the interaction sulfide phase/support without changing the stacking. A XAS study would be necessary to confirm this point.

4.3.2. Small Co clusters on the edges of sulfide slab

The presence of NTA, changing the interaction between Co and Mo as well as with alumina, could favor the growth of Co particles around the MoS_2 slabs. The presence of small CoS_x entities on the MoS_2 edge of conventional CoMo catalysts, which has already been proposed in the literature [32], could account for the increased CoMoS site concentration in the absence of a decrease of Mo site concentration and increase of sulfide-phase dispersion.

4.3.3. Formation of "(Co)MoSN"

The interaction between Co and nitrilo triacetic acid could lead to the insertion of some nitrogen in the sulfide slab and form some nitrogeno-sulfide sites as "CoMoSN" and "MoSN" at the edges of the MoS_2 slab. Data are available indicating the high activity of pure MoN and CoMoN catalysts, but also their high sensitivity to H_2S atmosphere [33–37]. One can estimate that the amount of N present as "CoMoSN" sites on the catalysts should be relatively low. This means that evidence of the interaction between Co and N would be difficult to discriminate from the interaction between Co and S using spectroscopic tools such as XPS and EXAFS. Unfortunately, IR spectroscopy of CO adsorption cannot detect such species as it has been shown that the ν(CO) bands on nitride and sulfide phases appear at almost the same wavenumbers (Table 2). The determination of the activity of pure nitride catalysts in the HYD and DDN routes for DMA decomposition could be a way to establish the formation of such "CoMoSN" species.

5. Conclusion

The addition of NTA to CoMo/alumina catalysts leads to a significant increase of thiophene HDS ($\times$2.6) and DMA HDN (HYD $\times$ 1.9) activities. By contrast, no effect is observed for liquid-phase DBT HDS, which shows the importance of the sulfidation and/or reaction conditions to obtain a positive NTA effect.

Increasing the amount of NTA in the CoMo catalysts progressively increases the spectral contribution of Co-promoted sites in the CO(ad)/IR measurements, up to an optimum for one mole of NTA for one mole of metals. A good correlation is observed between the rate of thiophene HDS and of DMA HYD, and this IR spectral contribution, suggesting that NTA significantly increases the total amount of Co-promoted sites.

However, there are strong indications that not only the number but also the quality of the Co-promoted sites changes upon addition of NTA. Firstly, while the TEM data show that the MoS_2 dispersion is not affected by NTA, no concomitant decrease in the number of unpromoted sites is observed in the CO(ad)/IR spectra. Secondly, parallel between catalytic and spectroscopic data shows unrealistic TOF. And thirdly, k(DDN) in the HDN of DMA increases more than proportionally with the increase of the spectral contribution of Co-promoted sites.

Three possibilities are considered to account for this change in CoMoS site quality: (i) increased formation of type II CoMoS slabs, (ii) formation of small Co(S) clusters on the edges of MoS_2 slabs, and (iii) formation of the so-called "CoMoSN" sites. Although, in view of the wider literature, (i) appears to be the most likely explanation, the combined body of our data does not allow discounting the other two.

Acknowledgments

M.A.L. thanks the CNRS and the Conseil Régional de Basse Normandie for supporting his PhD grant.

Appendix A. Supplementary material

Supplementary data associated with this article can be found, in the online version, at doi:10.1016/j.jcat.2009.07.006.

References

[1] H. Topsøe, B.S. Clausen, F.E. Massoth, in: J.R. Anderson, M. Boudard (Eds.), Hydrotreating Catalysis, Science and Technology, vol. 11, Springer-Verlag, Berlin/New York, 1996.
[2] J.A.R. van Veen, E. Gerkema, A.M. van der Kraan, P.A.J.M. Hendriks, H. Beens, J. Catal. 133 (1992) 112.
[3] S. Kasztelan, H. Toulhoat, J. Grimblot, J.P. Bonnelle, Appl. Catal. 13 (1984) 127.
[4] P. Da Silva, N.N. Marchal, S. Kasztelan, Stud. Surf. Sci. 106 (1997) 353.
[5] J.V. Lauritsen, J. Kibsgaard, G.H. Olesen, P.G. Moses, B. Hinnemann, S. Helveg, J.K. Nørskov, B.S. Clausen, H. Topsøe, E. Lægsgaard, F. Besenbacher, J. Catal. 249 (2007) 220–233.
[6] M.S. Thompson. 1986. U. Patent, Editor.
[7] S.L. Gonzalez-Cortés, T.-C. Xiao, P.M.F.J. Costa, B. Fontal, M.L.H. Green, Appl. Catal. A 270 (2004) 209.
[8] T. Shimizu, K. Hiroshima, T. Homna, T. Mochizuki, M. Yamada, Catal. Today 45 (1998) 271–276.
[9] K. Hiroshima, T. Mochizuki, T. Homna, T. Shimizu, M. Yamada, Appl. Surf. Sci. 121/122 (1997) 433.
[10] J.A.R. van Veen, H.A. Colijn, P.J.A.M. Hendricks, A.J. van Welsenes, Fuel. Proc. Technol. 35 (1993) 137.
[11] M.A. Lelias, J. van Gestel, F. Maugé, J.A.R. van Veen, Catal. Today 130 (2008) 109–116.
[12] E.J.M. Hensen, P.J. Kooyman, Y. van der Meer, A.M. van der Kraan, V.H.J. de Beer, J.A.R. van Veen, R.A. van Santen, J. Catal. 199 (2001) 224.
[13] Y. Okamoto, S.-Y. Ishihara, M. Kawano, M. Satoh, T. Kubota, J. Catal. 217 (2003) 12.
[14] T. Kubota, N. Hosomi, K.K. Bando, T. Matsui, Y. Okamoto, Phys. Chem. Chem. Phys. 5 (2003) 4510.
[15] L. Medici, R. Prins, J. Catal. 163 (1996) 38.
[16] A.M. de Jong, V.H.J. de Beer, J.A.R. van Veen, J.W. Niemantsverdriet, J. Phys. Chem. 100 (1996) 17722.
[17] L. Coulier, V.H.J. de Beer, J.A.R. van Veen, J.W. Niemantsverdriet, Topics in Catalysis 13 (2000) 99.
[18] L. Coulier, V.H.J. de Beer, J.A.R. van Veen, J.W. Niemantsverdriet, J. Catal. 197 (2001) 26.
[19] A.I. Dugulan, M.W.J. Crajé, G.J. Kearley, J. Catal. 222 (2004) 281–284.
[20] J.A.R. van Veen, E. Gerkema, A.M. Van der Kraan, A. Knoester, J. Chem. Soc. Chem. Commun. (1987) 1684.
[21] J. van Gestel, C. Dujardin, F. Maugé, J.C. Duchet, J. Catal. 202 (2001) 78–88.
[22] F. Maugé, J.C. Lavalley, J. Catal. 137 (1992) 69–76.
[23] F. Maugé, A. Vallet, J. Bachelier, J.C. Duchet, J.C. Lavalley, J. Catal. 162 (1996) 88–95.
[24] M.A. Lélias, J. van Gestel, F. Maugé, J.A.R. van Veen, Catal. Today 130 (2008) 109–116.
[25] P. Kooyman, J.A.R. van Veen, Catal. Today 130 (2008) 135.
[26] H.W. Zandbergen, P.J. Kooyman, A.D. van Langeveld, Proc. ICEM 14, Cancun, Mexico, 31 August–4 September 1998, Symposium W, vol. II (1998) 491.
[27] K. Inamura, K. Uchikawa, S. Matsuda, Y. Akai, Appl. Surf. Sci. 121/122 (1997) 468.
[28] H.R. Reinhoudt, C.H.M. Boons, A.D. van Langeveld, J.A.R. van Veen, S.T. Sie, J.A. Moulijn, Appl. Catal. A 207 (2001) 25.
[29] A. Travert, C. Dujardin, F. Maugé, E. Veilly, S. Cristol, J.F. Paul, E. Payen, J. Phys. Chem. B 110 (2006) 1261–1270.
[30] C. Dujardin, M.A. Lelias, J. van Gestel, A. Travert, J.C. Duchet, F. Maugé, Appl. Catal. A 322 (2007) 46–57.
[31] A.I. Dugulan, Ph,D, Thesis, Delft University, The Netherlands, 2008.
[32] Y. Okamoto, A. Kato, Usman, N. Rinaldi, T. Fujikawa, H. Koshika, I. Hiromitsu, T. Kubota, J. Catal. 265 (2009) 216–228.
[33] P.A. Aegerter, W.W.C. Quigley, G.J. Simpson, D.D. Ziegler, J.W. Logan, K.R. McCrea, S. Glazier, M.E. Bussell, J. Catal. 164 (1996) 109–121.
[34] S. Yang, C. Li, J. Xu, Q. Xin, J. Phys. Chem. B 102 (1998) 6986–6993.
[35] S.W. Yang, Y.X. Li, J. Xu, C. Li, Q. Xin, I. Rodriguez-Ramos, A. Guerrero-Ruiz, Phys. Chem. Chem. Phys. 2 (2000) 3313–3317.
[36] Z. Wu, A. Maroto-Valiente, A. Guerrero-Ruiz, I. Rodriguez-Ramos, C. Li, Q. Xin, Phys. Chem. Chem. Phys. 5 (2003) 1703–1707.
[37] Z. Wu, C. Li, Z. Wei, P. Ying, Q. Xin, J. Phys. Chem. B 106 (2002) 979–987.